Anthropogenic CO_2 warming challenged by 60-year cycle

François Gervais

Department of Physics, Faculty of Sciences & Techniques, François Rabelais University, Parc de Grandmont, 37200 Tours, France

ARTICLE INFO

ABSTRACT

Time series of sea-level rise are fitted by a sinusoid of period ~60 years, confirming the cycle reported for the global mean temperature of the earth. This cycle appears in phase with the Atlantic Multidecadal Oscillation (AMO). The last maximum of the sinusoid coincides with the temperature plateau observed since the end of the 20th century. The onset of declining phase of AMO, the recent excess of the global sea ice area anomaly and the negative slope of global mean temperature measured by satellite from 2002 to 2015, all these indicators sign for the onset of the declining phase of the 60-year cycle. Once this cycle is subtracted from observations, the transient climate response is revised downwards consistent with latest observations, with latest evaluations based on atmospheric infrared absorption and with a general tendency of published climate sensitivity. The enhancement of the amplitude of the CO_2 seasonal oscillations which is found up to 71% faster than the atmospheric CO_2 increase, focus on earth greening and benefit for crops yields of the supplementary photosynthesis, further minimizing the consequences of the tiny anthropogenic contribution to warming.

Contents

1. Introduction

A cycle of period ~60 years has been reported in global mean temperature of the earth (Schlesinger and Ramankutty, 1994; Ogurtsov et al., 2002; Klyashtorin and Lyubushin, 2003; Loehle, 2004; Zhen-Shan and Xian, 2007; Carvalo et al., 2007; Swanson and Tsonis, 2009; Scafetta, 2009; Akasofu, 2010; D'Aleo and Easterbrook, 2010; Loehle and Scafetta, 2011; Humlum et al., 2011; Chambers et al., 2012; Lüdecke et al., 2013; Courtillot et al., 2013; Akasofu, 2013; Macias et al., 2014; Ogurtsov et al., 2015). This cycle and others of smaller amplitude were found to be correlated with the velocity of the motion of the sun with respect to the center of mass of the solar system (Scafetta, 2009). This cycle is also in phase with AMO index (Knudsen et al., 2011; McCarthy et al., 2015). Section 2 will search for additional

signatures of this 60-year cycle in major components and sensitive indicators of climate. The impact on climate of the CO_2 emitted by burning of fossil fuels is a long-standing debate illustrated by 1637 papers found in the Web of Science by crossing the keywords

[anthropogenic] AND [greenhouse OR CO2] AND [warming]

This is to be compared to more than 1350 peer-reviewed papers which express reservations about dangerous anthropogenic CO_2 warming and/or insist on the natural variability of climate (Andrew, 2014). The transient climate response (TCR) is defined as the change in global mean surface temperature at the time of doubling of atmospheric CO_2 concentration. The range of uncertainty reported by AR5 (2013) is very wide, 1–2.5 °C. More recent evaluations, later than the publication of AR5 (2013), focus on low values lying between 0.6 °C and 1.4 °C (Harde, 2014; Lewis and Curry, 2014; Skeie et al., 2014; Lewis, 2015). The infrared absorption of CO_2 is well documented since

E-mail address: francois.gervais@univ-tours.fr.

the availability of wide-band infrared spectrometry (Ångström, 1900). Two infrared-active modes of the molecule are allowed by symmetry. The bending mode at the frequency $v = 20$ THz (wavelength 15 μm, wavenumber 667 cm^{-1}) is of crucial importance because it absorbs near the maximum of the blackbody radiation

$$B(v, T) = 2hv^3 \, n(v, T)/c^2 \qquad (1)$$

if T = 288 K, the mean surface temperature of the earth. $n(v,T) = (e^{hv/k_BT} - 1)^{-1}$ is the Bose-Einstein population factor, h the Planck constant, c the velocity of light and k_B the Boltzmann constant. The absorptivity of the earth's atmosphere is already 100% at the frequency of this bending mode. It is independent, therefore, of additional CO_2 concentration which increased from 0.03% to 0.04% by volume since the beginning of the industrial era. In the wavelength range from 14 to 16 μm, an atmospheric layer of thickness of ~100 m above the sea-level transmits less than 0.01% of the earth's radiation (Farmer, 1974; Barrett, 1995; Hug, 2000; Barrett et al., 2006), leaving very little earth radiation able to excite CO_2 molecules at higher altitudes. A higher CO_2 concentration assumes a smaller air thickness to reach opacity at 20 THz. To bypass this near saturation, the radiative-convective models (Manabe and Strickler, 1964) consider the infrared transmittance of an atmospheric layer no longer at the earth surface but at the top of the atmosphere (TOA) where it is no longer zero because the pressure is lower. Not only pressure but also temperature is lower due to the atmospheric lapse rate. With the aid of convective air currents which transport heat upward, anthropogenic CO_2 is considered in radiative-convective models to make the upper atmosphere cooler due to the lapse rate, because the altitude of the upper semi-transparent layer increases with CO_2 concentration. Myrhe et al. (1998) evaluated a radiative forcing of 5.35 LN(2) = 3.7 W/m² in case of CO_2 doubling. The factor 5.35 was estimated by comparing three radiative-convective models. The resulting warming would be.

$$\Delta T_{CO2\times2} = T_{EarthSurf}/4 \times \Delta F/R_{OLR} = 288/4 \times 3.7/238.5 = 1.1\ ^{\circ}C \qquad (2)$$

where $R_{OLR} = 238.5$ W/m² is the Output Long–wavelength Radiation (OLR) emitted by the earth/atm system at the TOA. Early versions of climatic models considered the *cooling* that the earth experienced from 1945 to 1970 and projected more cooling (Rasool and Schneider, 1971). After the onset of the temperature rise from 1980 to 1998, models abandoned dominant cooling by aerosols and rather insisted on CO_2 greenhouse warming. However Ring et al. (2012) recognize that the internal climate variability is primarily responsible for the early 20th century warming from 1910 to 1945 and for the subsequent cooling from 1945 to 1975. They focus on low values of climate sensitivity. The higher values and the large extension of the TCR uncertainty partly comes from the supposed positive feedbacks of water vapor and clouds which might increase $\Delta T_{CO2\times2}$ of Eq. (2) in the form.

$$\Delta T_{f=}\Delta T_{CO2\times2}/(1-f) \qquad (3)$$

if *f* is positive and lower than 1. Cloud tuning (Golaz et al., 2013) to achieve the desired radiation balance is a complementary cause of the dispersion of TCR. Positive feedbacks due to water vapor, the main infrared absorber of the thermal radiation emitted by the earth, were supposed to enhance warming, thus predicting «hot spots» under the tropics and at both poles. However, no «hot spot» is found in the high troposphere in subtropical regions (Douglass et al., 2004, 2008; Christy et al., 2010; Fu et al., 2011). In addition, at the altitude where the hot spots are expected, the humidity has decreased during the past 50 years, contrary to the assumption of increased water vapor giving rise to positive feedbacks. Even the total precipitable water slightly decreased since 1997 (see Fig. 4 of Vonder Harr et al., 2012), thus showing anticorrelation with an anthropogenic CO_2 increase of ~1/3 in the meantime. The polar amplification predicted by models (AR5, 2013)

will be discussed in Section 2. Conversely, Paltridge et al. (2009); Lindzen and Choi (2009, 2011); Spencer and Braswell (2010) focus on *negative* feedbacks assigned to increased albedo of additional clouds (Laken and Pallé, 2012) and/or to cooling effect of additional evaporation, lowering ΔT_f with respect to $\Delta T_{CO2 \times 2}$ in Eq. (3). Lindzen and Choi (2009, 2011) in particular exploited the observation of the variability of the radiative energy budget measured at the TOA which is not captured by models (Wielicki et al., 2002). If precipitating convective clouds cluster in larger clouds as temperature rise, negative feedbacks related to an iris effect are expected (Mauritsen and Stevens, 2015). The net effect of lowering of aerosol effects (Stevens, 2015) is a further reduction of TCR down to a medium estimate of 1.2 °C (Lewis, 2015). This would mean an almost cancelation of feedback parameter *f* in Eq. (3). Miskolczi (2007) considers a cancelation by negative feedbacks. More generally, salient features of atmospheric greenhouse gas theory have been questioned (Gerlich and Tscheuschner, 2009; Clark, 2010; Kramm and Dlugi, 2011). Atmospheric pressure at the surface and solar irradiance at the top of the atmosphere were shown to be the two sole parameters which are sufficient to determine accurately by dimensional analysis the surface temperature of six planets or satellites of the solar system (Volokin and ReLlez, 2015). This might mean the almost saturation of greenhouse effect (if any) or negative feedbacks in atmospheres which are so much different on Earth (0.04% of CO_2), the Moon (no atmosphere), Venus (96% of CO_2), Mars, Titan (a moon of Saturn), and Triton (a moon of Neptune). The controversy has reached a novel phase because, contrary to CMIP3 and CMIP5 warming projections (AR5, 2013), global mean temperatures at the surface of the earth display a puzzling « plateau » or « pause » or « hiatus » since the end of the last century (McKitrick, 2014). This hiatus seems to have encouraged climate modelers to refrain from exaggerated warming projections. This is illustrated by (i) a TCR upper limit lower in AR5 (2013) by 0.5 °C compared to AR4, (ii) lowest values of the 1–2.5 °C TCR range finally judged more likely in Fig. 11.25b of AR5 (2013), (iii) latest evaluations of TCR lying between 0.6 °C and 1.4 °C (Harde, 2014; Lewis and Curry, 2014; Skeie et al., 2014; Lewis, 2015), consistent with Eq. (2) and with the low side of AR5 (2013) TCR range. The tendency at lowering of both TCR and ECS (Equilibrium Climate Sensitivity) is illustrated in Fig. 1. A linear regression of published
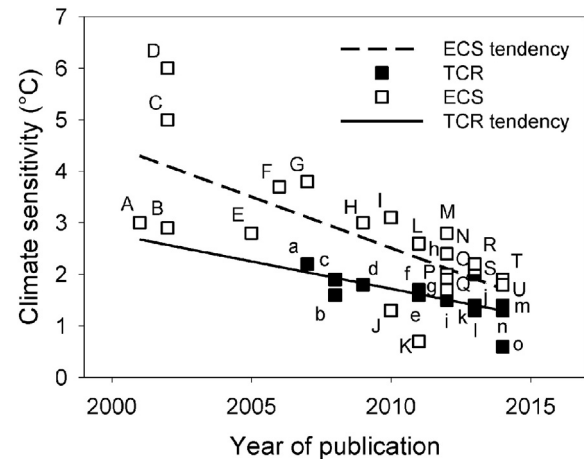

Fig. 1. Compilation of TCR and ECS climate sensitivity versus year of publication, complemented from the analyses of Lewis (2015) together with a linear regression of each set of data — A: Andronova and Schlesinger, 2001; B: Forest et al., 2002, C: Knutti et al., 2002, D: Gregory et al., 2002, E: Frame et al., 2005, F: Forest et al., 2006, G: Tomassini et al., 2007, H: Allen et al., 2009, I: Lin et al., 2010, J: Spencer and Braswell, 2010, K: Lindzen and Choi, 2011, L,e: Libardoni and Forest, 2011, M: Olsen et al., 2012, N,i: Schwartz, 2012, O,g: Aldrin et al., 2012, P: Ring et al., 2012, Q,h: Rogelj et al., 2012, R,k: Otto et al., 2013, S,l: Lewis, 2013, T: Skeie et al., 2014, U: Lewis and Curry, 2014, a: Stott and Forest, 2007, b: Knutti and Tomassini, 2008, c: Gregory and Forster, 2008, d: Meinshausen et al., 2009, f: Padilla et al., 2011, g: Gillett et al., 2012, j: Harris et al., 2013, m: Skeie et al., 2014, n: Lewis and Curry, 2014, o: Harde (2014).

data indicates a decrease of ECS by 0.2 °C yr.$^{-1}$ and a decrease of TCR by 0.1 °C yr.$^{-1}$. Wunsch and Heimbach (2014) analyzed ocean heat content down to abyssal depths with the aid of ARGO buoys and focus on anomalies also tinier than those published previously. They consider that the uncertainties on an oceanic warming reevaluated down to 0.0004 °C yr.$^{-1}$ remain too large to support the conjecture of heat supposed hidden in the oceans during the pause. The role of the sun on climate is emphasized (Le Mouel et al., 2009; Le Mouel et al., 2010; Lüdecke et al., 2013, 2015; Shaviv, 2015; Andrews et al., 2015). Owing to the importance of climatic projections for public policy decision making, challenged by the large TCR uncertainties which extend over 0.6–2.5 °C (AR5, 2013 complemented by Fig. 1), a ratio as large as 4.2, the purpose of this paper is to parameterize a major component of the natural variability of climate in Section 2 and, once this contribution is removed from observed climate change, to estimate in Section 3 which fraction remains attributable to the warming of residual anthropogenic CO_2. Results will be compared with latest detailed evaluations of warming due to infrared absorption of atmosphere as a function of altitude and latitude (Harde, 2014), published after AR5 (2013). The benefit for mankind of the favorable impact on crops yields of the enhanced photosynthesis of anthropogenic CO_2 parameterized via the evolution of the amplitude of seasonal oscillations will be discussed by comparison with the risk of dangerous additional CO_2 warming in Section 4.

2. 60-year cycle confirmed in sea-level rise and global sea ice area

Fig. 2(a) shows the time series of the sea-level rise. Both thin dotted curves reproduce the upper and lower limits of the uncertainty range of tide gauge data analyzed by three groups of authors (Jevrejeva et al., 2006; Church and White, 2011; Ray and Douglas, 2011), as reproduced from Fig. 3.14 of AR5 (2013). The arithmetic mean of both upper and lower curves is complemented after 1992 by more recent smoothed tide gauge data (Jevrejeva et al., 2014). The heavy full curve is a regression with a sinusoidal wave form. A period of 62 years is deduced. This global approach confirms the local oscillations with a period around 60 years reported for a majority of tide gauges (Chambers et al., 2012). Once this cycle is removed, the average global sea level rise is 1.7–1.8 mm yr.$^{-1}$ as given by tide gauges (NOAA-tide, 2015), consistent with Fig. 2(a). The periods found for the cycles of sea-level rise is found similar to the one which fits unfiltered HadCRUT4 (2014) global mean temperature anomaly in Fig. 2(b), where the sinusoid is added to a linear contribution of 0.006 °C yr.$^{-1}$ since 1880. This linear increase is consistent with the latest ascending tangent to the ~248 years cycle reported by Lüdecke et al. (2015), confirming previous analyses by De Vries (1958) and Suess (1980). The positions of the extremes in Fig. 2 appear close enough to strongly suggest two signatures of the same cycle. The amplitude of the sinusoidal contribution in Fig. 2(b) also appears compatible with the amplitude of the cycle of sea-level rise in Fig. 2(a) via thermal expansion. This cycle is synchronous with the Atlantic multidecadal oscillation parameterized via the AMO index (Knudsen et al., 2011; McCarthy et al., 2015). The time series of the ocean heat content anomaly and of the earth's radiation imbalance (Douglass and Knox, 2009) also appear compatible with this 60-year cycle. Fig. 3 shows the global sea ice area anomaly measured since the beginning of the satellite era. Daily data of both hemispheres are added by the Polar Research Group of the University of Illinois (UIUC, 2015), here summed over each year. The remarkable change of tendency observed in 2013 and 2014 is to be emphasized. Data are in excess of the mean, contrary to the deficit observed during the previous decade. This is noticeable not only because global sea ice area is a sensitive indicator of climate, in particular in view of the polar amplification predicted by models (AR5, 2013), but also because the change of sign of the anomaly contributes to an increase of the earth albedo and, therefore, to a cooling component. The recent excess of global sea ice area/extent anomaly, comes from the addition of two tendencies. (i) A continuous increase of the Antarctic sea ice area/extent anomaly is
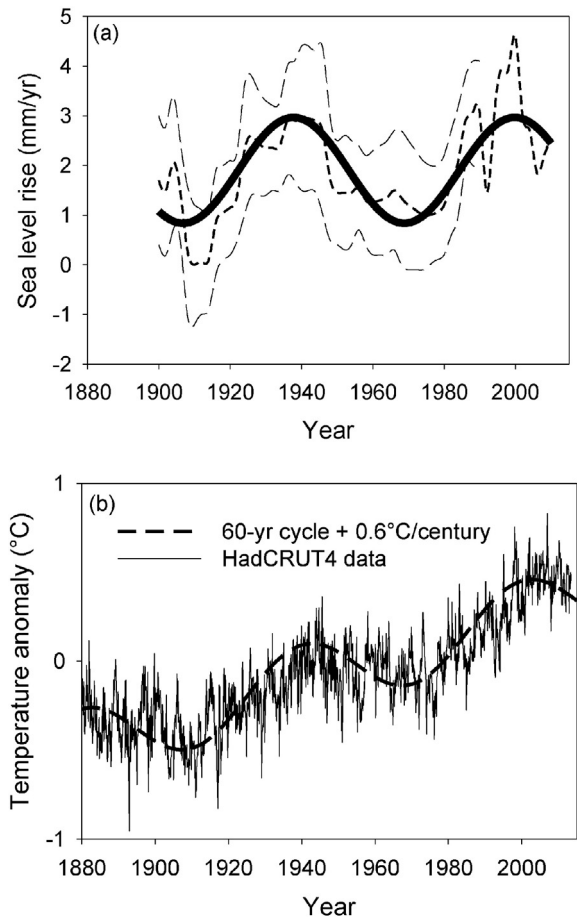

observed. The sea ice extent reached a record high of 20.14 millions of km^2 on September 21, 2014. (ii) The Arctic sea ice area anomaly recovered after the minimum observed at the end of the summer 2012. As a result of this change of tendency confirmed by temperature data at low latitudes (Gleisner et al., 2015), instead of the linear regression currently displayed, a regression with a sinusoid has been tried. Results are

Fig. 2. (a) Time series of upper and lower uncertainty bars (thin dotted curves) of tide gauge data reproduced from Fig. 3.14 of AR5 (2013). The heavy full curve is a regression by a sinusoid of period 62 years of the arithmetic mean complemented after 1992 by smoothed tide gauge data of Jevrejeva et al. (2014). (b) A fit of a cycle of period 60 years added to a straight line of slope 0.6 °C per century to HadCRUT4 (2014) global mean temperature data.
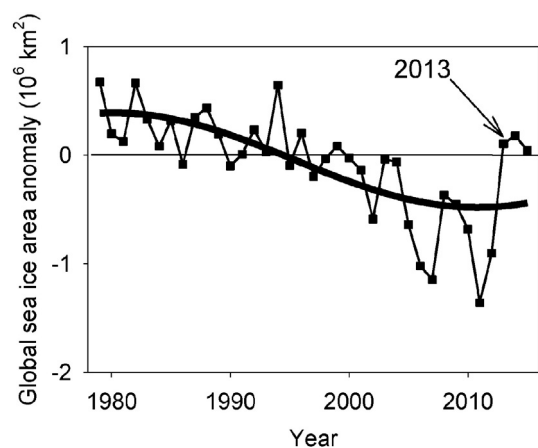

Fig. 3. Global sea ice area anomaly (UIUC, 2015) and regression (full curve) by a sinusoid of period 61 years. The data point of 2015 integrates data up to August 9.

shown in Fig. 3. Half a cycle is found from which a period of 61 years is extracted, consistent with Fig. 2. Temperatures measured at northern latitudes 64°–90°N displayed in the upper part of Fig. 7 of Hansen and Lebedeff (1987) show a maximum around 1940 and a minimum around 1970, suggesting a previous minimum of Arctic sea ice around 1940, consistent with Fig. 3. Note that because the Antarctic sea ice area anomaly increased continuously, the sinusoidal component of Fig. 3 comes from the Arctic contribution, itself consistent with AMO index. The last maximum observed since the end of the 20th century in Fig. 2, confirmed by the minimum of global sea ice area anomaly in Fig. 3, provides a straightforward understanding of the temperature plateau without the need to invoke other factors such as a change of earth albedo related to aerosols emitted by volcanic eruptions, or other natural phenomena which are ruled out because they are random, not cyclic. Besides, the four following indicators sign for the onset of the declining phase of the 60-year cycle.

(i). The recent change of sign of global sea ice area anomaly which reveals an excess in Fig. 3, a sensitive indicator of climate, is unexpected from model projections (AR5, 2013).

(ii). The AMO index indicates the onset of a declining phase.

(iii). A negative temperature slope is measured from 2002 to 2015 independently by different satellites in the low troposphere by Remote Sensing System (RSS, 2015) and by UAH (Spencer et al., 2015) as shown in Fig. 4. The plot is voluntarily restricted to 13 years, viz. less than 1/4 of the 60 year-cycle, to evaluate the sign of the tangent to the sinusoid.

(iv). A deceleration of the sea-level rise measured by satellite altimetry is also found since 2002 (Chen et al., 2014; Cazenave et al., 2014).

3. Anthropogenic CO$_2$ warming

The average CO$_2$ increase in the atmosphere, measured accurately by infrared spectrometry at Mauna Loa (NOAA, 2015), is 1.99 part per million (ppm) per year from 1995 to 2014, viz. 1.99/400 = 0.5% yr.$^{-1}$. The largest yearly increase observed in 1998, nearly 3 ppm, *followed* the largest El Niño warm fluctuation by 10 months. Other CO$_2$ increases above the mean such as 2.52 ppm in 2005, 2.42 ppm in 2010, 2.65 ppm in 2012 or 2.28 ppm in 2014, also follow by 9–11 months (Humlum et al., 2013) El Niño temperature fluctuations parameterized via the Multivariate ENSO (El Niño Southern Oscillation) index (MEI,
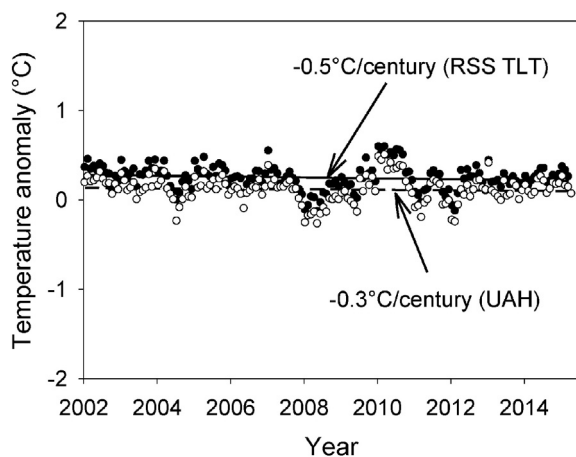

Fig. 4. Linear regression of RSS TLT (RSS, 2015) and UAH LT (Spencer et al., 2015) earth surface temperature anomaly measured by different satellites, independently. To corroborate the estimate of the tangent to the sinusoid of Fig. 2(b) during the latest years, 13 years are chosen here because the time series has to be as long as possible but remain shorter that 1/4 of the 60-year cycle. Both slopes show a *negative* sign which confirms each other.

2014). The relationship is confirmed for negative MEI indices which correspond to La Niña fluctuations such as those in 1999–2001 or 2008. They match low CO$_2$ yearly increases of 0.93–1.6 ppm and 1.6 ppm, respectively. However, the apparent correlation of yearly CO$_2$ increases with MEI or with Southern Oscillation Index (SOI) (Zeng et al., 2005) is questioned by the case of the year 1992 which shows a yearly CO$_2$ increase 7 *times smaller* than the largest one of 1998 whereas the MEI was *positive* due to El Niño. The earth indeed experienced in 1992 a temperature drop as large as − 0.5 °C due to the aerosols emitted by the eruption of Mount Pinatubo volcano which momentarily attenuated the solar flux. The correlation of yearly CO$_2$ increase, therefore, appears not with MEI or SOI but with *global mean temperature* to which El Niño and La Niña contribute. This temperature/CO$_2$ correlation may be tentatively explained, at least partly, by the solubility of CO$_2$ into water which decreases with temperature, consistent with sea pH maps (Byrne et al., 2010). Warm temperature fluctuations favor CO$_2$ release from the oceans which contain 60 times more CO$_2$ than the atmosphere (AR5, 2013), whereas cooler fluctuations favor its oceanic capture. The very small CO$_2$ increase of 0.14% yr.$^{-1}$ observed in 1992 might be viewed as an upper estimate of the residual anthropogenic addition in the atmosphere after action of carbon sinks favored by low temperatures. The correlation of yearly CO$_2$ increases with temperature fluctuations, and their lag of several months (Humlum et al., 2013) were discussed elsewhere (Park, 2009; Beenstock et al., 2012, Salby, 2012, Gervais, 2014). Note that the decrease of oceanic alkalinity (pH ~ 8) due to the increased CO$_2$ partial pressure has been reported as ΔpH = − 0.0017 yr.$^{-1}$ (Byrne et al., 2010). By using latest TCR findings (Harde, 2014; Lewis and Curry, 2014; Skeie et al., 2014; Lewis, 2015) consistent with Eq. (2), with the lowest value of the TCR range considered more likely in Fig. 11.25b (AR5, 2013) and with the tendency of Fig. 1, an anthropogenic warming of

$$(0.6\text{–}1.4\ °C) \times (0.0014\text{–}0.005\ \text{yr}^{-1}) \times 85\ \text{yrs} = 0.1\text{–}0.6\ °C$$

is extrapolated in 2100. The purpose of this crude estimate is to focus on the same order of magnitude as the natural variability through parameters extracted from Fig. 2(b). The temperature increase in each ascending phase of the cycle in the 1930s and in the 1990s, indeed is 0.6 °C as shown in Fig. 2(b) although CO$_2$ emissions were ~6 times lower in the 1930s compared to the 1990s. CMIP3 and CMIP5 climate models which fit data in the second ascending phase conversely are unable to reproduce the observations in the first ascending phase from 1910 to 1940 as shown in Fig. TS.9(a) of AR5 (2013) and after 1998. The slope of the linear contribution observed since 1880 in Fig. 2(b) is 0.6 °C per century although CO$_2$ emissions have been multiplied by ~10 in the meantime. In particular, no detectable change of slope is found before and after the onset of large CO$_2$ emissions around 1950.

Fig. 5 reproduces the TLS channel temperature measured by RSS (2015) in the low stratosphere (LS) plotted versus atmospheric CO$_2$ concentration (NOAA, 2015). The plot concentrates on the past 22 years because (i) the previous period displayed in the inset shows peaks related to major volcanic eruptions which complicate the analysis, (ii) 22 years correspond to not less than 50% of the CO$_2$ increase since 1959 measured accurately at Mauna Loa (NOAA, 2015) and to ~40% of the CO$_2$ increase estimated since the beginning of the industrial era. In spite of this large CO$_2$ increase, no temperature change is observed after 1993, although it is measured at the altitude where the most marked signature of temperature change predicted by radiative–convective models is expected. Models indeed expect a temperature change as large as 6.6 °C just above the tropopause in case of CO$_2$ increase from 280 ppm to 400 ppm (Sloan and Wolfendale, 2013, see in particular their Fig. 1). Contrary to this prediction, the LS hiatus is found to extend over 23 years, even longer than the LT hiatus. Recent detailed evaluations based on the infrared absorption of atmosphere at different latitudes, altitudes and pressures, reported 0.2 °C for the anthropogenic warming during the twentieth century (Harde, 2014). This
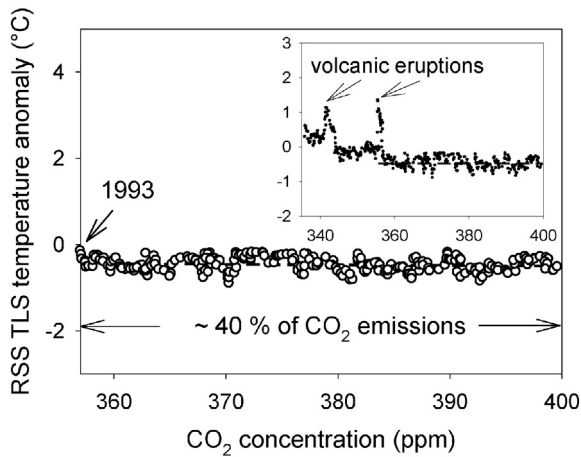
Fig. 5. Plateau of RSS (2015) TLS temperature measured by satellite in the low stratosphere since 1993 (the inset shows all available data) plotted versus atmospheric CO_2 concentration (NOAA 2015) showing the absence of discernible correlation in a period corresponding to not less than ~40% of all the CO_2 emitted since the beginning of the industrial era.

Fig. 6. Increase by 36% of the amplitude of the seasonal northern–hemisphere spring–summer drop of CO_2 atmospheric concentration measured at La Jolla, California (SCRIPPS, 2014). This enhancement is 71% faster than the increase of atmospheric CO_2 concentration, 21%, over the same period.

is consistent with a minor fraction of the slope of 0.6 °C per century of the linear contribution found since 1880 from the fit to Fig. 2(b). The remaining is attributable to the variability of the solar irradiance and to mechanisms which may amplify it (Le Mouel et al., 2009, 2010; Lüdecke et al., 2013, 2015; Shaviv, 2015). The key points of Harde (2014) deal with several mechanisms pointing towards the almost saturation of CO_2 warming. In particular, since the CO_2 infrared linewidth is broadened by pressure in the low troposphere, there is no earth radiation left for the wings of *narrower* lines at the TOA because it is absorbed below. In addition, the overlap of the CO_2 band at 20 THz and of the water vapor spectrum minimizes the additional absorption. Harde (2014) reports a warming of 0.6 ± 0.1 °C in case of CO_2 doubling. This is consistent with the absence of temperature change for the CO_2 concentration range displayed in Fig. 5, whereas a TCR much larger would be hardly compatible with observations. At the present rate of 0.005 yr.$^{-1}$ of CO_2 increase, a TCR of 0.6 °C implies a warming of ~0.3 °C in 2100. This is so tiny compared for example to the diurnal or seasonal temperature variability, or to that related to latitude, that the replacement of the observed mean value of 0.005 yr.$^{-1}$ by the estimate of anthropogenic residual of 0.0014 yr.$^{-1}$ observed in 1992 would not much change the conclusions.

4. Enhancement of amplitude of CO_2 seasonal oscillations

Fig. 6 illustrates the increase of the amplitude of the CO_2 seasonal oscillations measured in 2013 compared to early measurements of 1969 at La Jolla, California (SCRIPPS, 2014). The drop of CO_2 concentration experienced each year from May to August is the signature of the amplitude of the spring–summer enhanced photosynthesis in the northern hemisphere (where the vegetation area is larger than in the southern hemisphere). The amplitude of the seasonal oscillation is found very small in the Antarctic for lack of surrounding vegetation (SCRIPPS, 2014). It is medium at Mauna Loa in the middle of the Pacific Ocean. It is larger in green areas. The increase of the amplitude observed in 2013 compared to 1969 in Fig. 6, is found up to 36% larger. The CO_2 content measured at Mauna Loa increased by 21% in the meantime. The point which seems to be of importance is that the ratio of both increases is 36/21 = 1.71 with no precursor sign of saturation, meaning that the amplitude of the seasonal oscillation increased 71% *faster* than that of the atmospheric CO_2. This illustrates how much flora appreciates this food supplement, as confirmed by other methods (Bellassen et al., 2011; Clay et al., 2012; Pretzsch et al., 2014). The whole earth is growing greener as also observed from space. The benefit of additional CO_2 even concerns arid
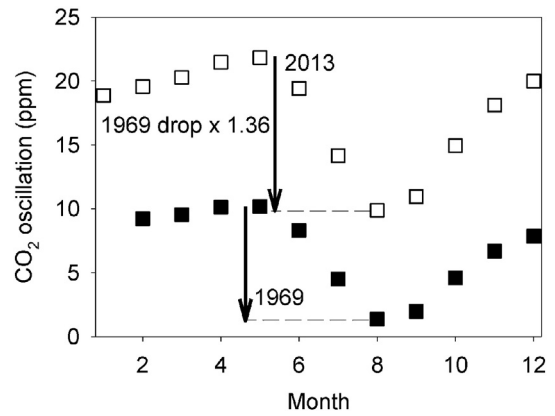
areas (Metcalfe, 2014). Amplified fertilization of nutritive plants by additional photosynthesis related to the CO_2 increase at the present rate of 2/400 = 0.5% yr.$^{-1}$ is to be emphasized since it is already exploited in CO_2-enriched greenhouses. The profit for mankind since 1961 has been estimated to $3.2 trillions over the period from 1961 to 2011 (CO2Science, 2013 and references therein which detail the benefit for nutritive plants).

5. Summary

Dangerous anthropogenic warming is questioned (i) upon recognition of the large amplitude of the natural 60–year cyclic component and (ii) upon revision downwards of the transient climate response consistent with latest tendencies shown in Fig. 1, here found to be at most 0.6 °C once the natural component has been removed, consistent with latest infrared studies (Harde, 2014). Anthropogenic warming well below the potentially dangerous range were reported in older and recent studies (Idso, 1998; Miskolczi, 2007; Paltridge et al., 2009; Gerlich and Tscheuschner, 2009; Lindzen and Choi, 2009, 2011; Spencer and Braswell, 2010; Clark, 2010; Kramm and Dlugi, 2011; Lewis and Curry, 2014; Skeie et al., 2014; Lewis, 2015; Volokin and ReLlez, 2015). On inspection of a risk of anthropogenic warming thus toned down, a change of paradigm which highlights a benefit for mankind related to the increase of plant feeding and crops yields by enhanced CO_2 photosynthesis is suggested.

Acknowledgement

References

Akasofu, S.I., 2010. On the recovery from the Little Ice Age. Nat. Sci. 2, 1211.
Akasofu, S.I., 2013. On the present halting of global warming. Climate 1, 4.
Aldrin, M., Holden, M., Guttorp, P., Skeie, R.B., Myhre, G., Berntsen, T.K., 2012. Bayesian estimation of climate sensitivity based on a simple climate model fitted to observations of hemispheric temperatures and global ocean heat content. Environmetrics 23, 253–271.
Allen, M.R., Frame, D.J., Huntingford, C., Jones, C.D., Lowe, J.A., Meinshausen, M., Meinshausen, N., 2009. Warming caused by cumulative carbon emissions towards the trillionth tonne. Nature 458, 1163–1166.
Andrew, K., 2014. www.populartechnology.net/2009/10/peer-reviewed-papers-supporting.html.
Andrews, M.B., Knight, J.R., Gray, L.J., 2015. A simulated lagged response of the North Atlantic Oscillation to the solar cycle over the period 1960–2009. Environ. Res. Lett. 10, 054022.
Andronova, N.G., Schlesinger, M.E., 2001. Objective estimation of the probality density function for climate sensitivity. J. Geophys. Res. 106, 22605–22611.

Ångström, K., 1900. Über die bedeutung des wasserdampfes und der kohlensäure bei der absorption der erdatmosphäre. Ann. Phys. 308, 720.

AR5, 2013. Climate change 2013: the physical science basis. In: Stocker, T.F., Qin, D., Plattner, G.-K., Tignor, M.M., Allen, S.K., Boschung, J., Nauels, A., Xia, Y., Bex, V., Midgley, P.M. (Eds.), Contribution of Working Group I to the Fifth Assessment Report of the Intergovernmental Panel on Climate Change. Cambridge University Press, Cambridge, United Kingdom and New York, NY, USA.

Barrett, J., 1995. The roles of carbon dioxide and water vapour in warming and cooling the earth's troposphere. Spectrochim. Acta A 51, 415.

Barrett, J., Bellamy, D., Hug, H., 2006. On the sensitivity of the atmosphere to the doubling of the carbon dioxide concentration and on water vapor feedback. Energy Environ. 17, 603.

Beenstock, M., Reingewertz, Y., Paldor, N., 2012. Polynomial cointegration tests of anthropogenic impact on global warming. Earth Syst. Dyn. 3, 173–188.

Bellassen, V., Viovy, N., Luyssaert, S., Le Marie, G., Schelhaas, M.-J., Ciais, P., 2011. Reconstruction and attribution of the carbon sink of European forests between 1950 and 2000. Glob. Chang. Biol. 17, 3274.

Byrne, R.H., Mecking, S., Feely, R.A., Liu, X.W., 2010. Direct observations of basin-wide acidification of the North Atlantic Pacific ocean. Geophys. Res. Lett. 37, L02601.

Carvalo, L.M.V., Tsonis, A.A., Jones, C., Rocha, H.R., Polito, P.S., 2007. Anti-persistence in the global temperature anomaly field. Nonlinear Process. Geophys. 14, 723.

Cazenave, A., Dieng, H.B., Meyssignac, B., Von Schuckmann, K., Decharme, B., Berthier, E., 2014. The rate of sea-level rise. Nat. Clim. Chang. 4, 358.

Chambers, D.P., Merryfield, M.A., Nerem, R.S., 2012. Is there a 60-year oscillation in global mean sea-level? Geophys. Res. Lett. 39, L18607.

Chen, X., Feng, Y., Huang, N.E., 2014. Global sea-level trend during 1993–2012. Glob. Planet. Chang. 112, 26.

Christy, J.R., Herman, B., Pielke Sr., R., Klotzback, P., McNider, R.T., Hnilo, J.J., Spencer, R.W., Chase, T., Douglass, D., 2010. What do observational datasets say about modeled tropospheric temperature trends since 1979? Remote Sens. 2, 2148.

Church, J.A., White, N.J., 2011. Sea-level rise from the late 19th to the early 21st century. Surv. Geophys. 32, 585.

Clark, R., 2010. A null hypothesis for CO_2. Energy Environ. 21, 171.

Clay, D.E., Carlson, G.C., Clay, S.A., Stone, J., Reitsma, K.D., Gelderman, R.H., 2012. Publication of the International Plant Nutrition Institute: Better Crops. 96 pp. 20–22 (www.ipni.net/publication/bettercrops.nsf/0/7626A849E98D2AB106257A090060E697/$FILE/Better Crops 2012–2 p.20.pdf).

CO2Science, 2013. http://www.co2science.org/education/reports/co2benefits/MonetaryBenefitsofRisingCO2onGlobalFoodProduction.pdf.

Courtillot, V., Le Mouël, J.L., Kossobokov, V., Gibert, D., Lopes, F., 2013. Multi-decadal trends of global surface temperature: a broken line with alternating ~30 yr linear segments? Atmos. Clim. Sci. 3, 364.

D'Aleo, J., Easterbrook, D.J., 2010. Multidecadal tendencies in Enso and global temperatures related to multidecadal oscillations. Energy Environ. 21, 436.

De Vries, H., 1958. Variation in concentration of radiocarbon with time and location on Earth. K. Ned. Akad. Van. Wet. B 61, 94–102.

Douglass, D.H., Knox, R.S., 2009. Ocean heat content and Earth's radiation inbalance. Phys. Lett. A 373, 3296.

Douglass, D.H., Christy, J.R., Pearson, B.D., Singer, S.F., 2008. A comparison of tropical temperature trends with model predictions. Int. J. Climatol. 28, 1693.

Douglass, D.H., Pearson, B.D., Singer, S.F., 2004. Altitude dependence of atmospheric temperature trends: climate models versus observation. Geophys. Res. Lett. 31, L13208.

Farmer, V.C., 1974. Infrared Spectra of Minerals, Ed. Mineralogical society of Great Britain and Ireland, London.

Forest, C.E., Stone, P.H., Sokolov, A.P., 2006. Estimated PDFs of climate system properties including natural and anthropogenic forcings. Geophys. Res. Lett. http://dx.doi.org/10.1029/2005GL023977.

Forest, C.E., Stone, P.H., Sokolov, A.P., Allen, M.R., Webster, M.D., 2002. Quantifying uncertainties in climate system properties with the use of recent climate observations. Science 295, 113–117.

Frame, D.J., Booth, B.B.B., Kettleborough, J.A., Stainforth, D.A., Gregory, J.M., Collins, M., Allen, M.R., 2005. Constrained climate forecasts: the role of prior assumptions. Geophys. Res. Lett. http://dx.doi.org/10.1029/2004GL022241.

Fu, Q., Manabe, S., Johanson, C.M., 2011. On the warming in the tropical upper troposphere: models versus observations. Geophys. Res. Lett. 38, L15704.

Gerlich, G., Tscheuschner, R.D., 2009. Falsification of the atmospheric CO_2 Greenhouse effects within the frame of physics. Int. J. Mod. Phys. B 23, 275–224 (1333).

Gervais, F., 2014. Tiny warming of residual anthropogenic CO_2. Int. J. Mod. Phys. B 28, 1450095.

Gillett, N.P., Arora, V.K., Flato, G.M., Scinocca, J.F., von Salzen, K., 2012. Improved constraints on 21st-century warming derived using 160 years of temperature observations. Geophys. Res. Lett. 39, L01704.

Gleisner, H., Thejll, P., Christiansen, B., Nielsen, J.K., 2015. Recent global warming hiatus dominated by low-latitude temperature trends in surface and troposphere data. Geophys. Res. Lett. http://dx.doi.org/10.1002/2014GL062596.

Golaz, J.-C., Horowitz, L.W., Levy, H., 2013. Cloud tuning in a coupled climate model: Impact on 20th century warming. Geophys. Res. Lett. 40, 2246.

Gregory, J.M., Forster, P.M., 2008. Transient climate response estimated from radiative forcing and observed temperature change. J. Geophys. Res. Atmos. 113, D23105.

Gregory, J.M., Stouffer, R.J., Raper, S.C.B., Stott, P.A., Rayner, N.A., 2002. An observationally based estimate of the climate sensitivity. J. Clim. 15, 3117–3121.

HadCRUT4, 2014. http://www.metoffice.gov.uk/hadobs/hadcrut4.

Hansen, J., Lebedeff, S., 1987. Global trends of measured surface air temperature. J. Geophys. Res. 92, 13345.

Harde, H., 2014. Advanced two-layer climate model for the assessment of global warming by CO_2. Open J. Atmos. Clim. Chang. http://dx.doi.org/10.15764/ACC.2014.03001.

Harris, G.R., Sexton, D.M.H., Booth, B.B.B., Collins, M., Murphy, J.M., 2013. Probabilistic projections of transient climate change. Clim. Dyn. http://dx.doi.org/10.1007/s00382–012–1647-y.

Hug, H., 2000. A critical review of the hypothesis that climate change is caused by carbon dioxide. Energy Environ. 11, 631.

Humlum, O., Solheim, J.-H., Stordahl, K., 2011. Identifying natural contributions to late Holocene climate change. Glob. Planet. Chang. 79, 145.

Humlum, O., Stordahl, K., Solheim, J.E., 2013. The phase relation between atmospheric carbon dioxide and global temperature. Glob. Planet. Chang. 100, 51.

Idso, S.B., 1998. CO_2-induced global warming: a skeptic's view of potential climate change. Clim. Res. 10, 69.

Jevrejeva, S., Grinsted, A., Moore, J.C., Holgate, S.J., 2006. Nonlinear trends and multi-year cycles in sea-level records. Geophys. Res. 111, C09012.

Jevrejeva, S., Moore, J.C., Grinsted, A., Matthews, A.P., Spada, G., 2014. Trends and acceleration in global and regional sea-levels since 1807. Glob. Planet. Chang. 113, 11.

Klyashtorin, L.B., Lyubushin, A.A., 2003. On the coherence between dynamics of the world fuel consumption and global temperature anomaly. Energy Environ. 14, 773.

Knudsen, M.F., Seidenkrantz, M.-S., Jacobsen, B.H., Kuijpers, A., 2011. Tracking the Atlantic multidecadal oscillation through the last 8,000 years. Nat. Commun. http://dx.doi.org/10.1038/ncomms1186.

Knutti, R., Tomassini, L., 2008. Constraints on the transient climate response from observed global temperature and ocean heat uptake. Geophys. Res. Lett. 35, L09701.

Knutti, R., Stocker, T.F., Joos, F., Plattner, G.K., 2002. Constraint on radiative forcing and future climate change from observations and climate model ensembles. Nature 416, 719–723.

Kramm, G., Dlugi, R., 2011. Scrutinizing the atmospheric greenhouse effect and its climatic impact. Nat. Sci. 3, 971.

Laken, P.A., Pallé, E., 2012. Understanding sudden changes in cloud amount: the Southern annular mode and South American weather fluctuations. J. Geophys. Res. 117, D13103.

Le Mouel, J.-L., Blanter, E., Shnirman, M., Courtillot, V., 2009. Evidence for solar forcing in variability of temperatures and pressures in Europe. J. Atmos. Sol. Terr. Phys. 71, 1309.

Le Mouel, J.-L., Blanter, E., Shnirman, M., Courtillot, V., 2010. Solar forcing of the semi-annual variation of length-of-day. Geophys. Res. Lett. 37, L15307.

Lewis, N., 2013. An objective Bayesian, improved approach for applying optimal fingerprint techniques to estimate climate sensitivity. J. Clim. 26, 7414–7429.

Lewis, N., 2015. Pitfalls in climate sensitivity estimation. WCRP Grand Challenge Workshop: Earth's Climate Sensitivities, Rindberg (Germany).

Lewis, N., Curry, J.A., 2014. The implications for climate sensitivity of AR5 forcing and heat uptake estimates. Clim. Dyn. http://dx.doi.org/10.1007/s00382–014-2342-y.

Libardoni, A.G., Forest, C.E., 2011. Sensitivity of distributions of climate system properties to the surface temperature dataset. Geophys. Res. Lett. http://dx.doi.org/10.1029/2011GL049431.

Lin, B., et al., 2010. Estimation of climate sensitivity based on top-of-atmosphere radiation imbalance. Atmos. Chem. Phys. 10, 1923–1930.

Lindzen, R.S., Choi, Y.S., 2009. On the determination of climate feedbacks from ERBE data. Geophys. Res. Lett. 36, L16705.

Lindzen, R.S., Choi, Y.S., 2011. On the observational determination of climate sensitivity and its implications. Asia-Pac. J. Atmos. Sci. 47, 377.

Loehle, C., 2004. Climate change: detection and attribution of trends from long-term geologic data. Ecol. Model. 171, 433.

Loehle, C., Scafetta, N., 2011. Climate change attribution using empirical decomposition of. climatic data. Open Atmos. Sci. J. 5, 74.

Lüdecke, H.-J., Hempelmann, A., Weiss, C.O., 2013. Multi-periodic climate dynamics: spectral analysis of long-term instrumental and proxy temperature records. Clim. Past 9, 447.

Lüdecke, H.-J., Weiss, C.O., Hempelmann, A., 2015. Paleoclimate forcing by the solar De Vries/Suess cycle. Clim. Past Discuss. 11, 279–305.

Macias, D., Stips, A., Garcia-Gorriz, E., 2014. Application of the singular spectrum analysis technique to study the recent hiatus on the global surface temperature record. PLoS ONE 9, e107222.

Manabe, S.R., Strickler, R.F., 1964. Thermal equilibrium of the atmosphere with a convective adjustment. J. Atmos. Sci. 21, 361.

Mauritsen, T., Stevens, B., 2015. Missing iris effect as a possible cause of muted hydrological change and high climate sensitivity in models. Nat. Geosci. http://dx.doi.org/10.1038/NGEO2414.

McCarthy, G.D., Haigh, I.D., Hirschi, J.J.-M., Grist, J.P., Smeed, D.A., 2015. Ocean impact on decadal Atlantic climate variability revealed by sea-level observations. Nature http://dx.doi.org/10.1038/nature14491.

McKitrick, R.R., 2014. HAC-robust measurement of the duration of a trendless subsample in a global climate time series. Open J. Stat. 4, 527.

MEI, 2014. http://www.esrl.noaa.gov/psd/enso/mei.

Meinshausen, M., et al., 2009. Greenhouse-gas emission targets for limiting global warming to 2 °C. Nature 458, 1158–1162.

Metcalfe, B.B., 2014. Climate science: a sink down under. Nature 509, 566.

Miskolczi, F., 2007. Greenhouse effect in semi-transparent planetary atmospheres. Q. J. Hung. Meteorol. Serv. 111, 1.

Myrhe, G., Highwood, E.J., Shine, K.P., Stordal, F., 1998. New estimates of radiative forcing due to well mixed greenhouse gases. Geophys. Res. Lett. 25, 2715.

NOAA, 2015. http://www.esrl.noaa.gov/gmd/ccgg/trends.

NOAA-tide, 2015. http://tidesandcurrents.noaa.gov/sltrends/globalregional.htm.

Ogurtsov, M., Lindholm, M., Jalkanen, R., Veretenenko, S., 2015. Evidence for the Gleissberg solar cycle at the high-latitudes of the Northern Hemisphere. Adv. Space Res. 55, 1285–1290.

Ogurtsov, M.G., Nagovitsyn, Y.A., Kocharov, G.E., Jungner, H., 2002. Long-period cycles of the sun's activity recorded in direct solar data and proxies. Sol. Phys. 211, 371.

Olsen, R., Sriver, R., Goes, M., Urban, N.M., Matthews, H.D., Haran, M., Keller, K., 2012. A climate sensitivity estimate using Bayesian fusion of instrumental observations and an earth system model. Geophys. Res. Lett. http://dx.doi.org/10.1029/2011JD016620.

Otto, A., et al., 2013. Energy budget constrains on climate response. Nat. Geosci. 6, 415–416.

Padilla, L.E., Vallis, G.K., Rowley, C.W., 2011. Probabilistic estimates of transient climate sensitivity subject to uncertainty in forcing and natural variability. J. Clim. 24, 5521–5537.

Paltridge, G., Arking, A., Pook, M., 2009. Trends in middle- and upper-level tropospheric humidity from NCEP reanalysis data. Theor. Appl. Climatol. 98, 351.

Park, J., 2009. A re-evaluation from the coherence between global-average atmospheric CO_2 and temperatures at interannual time scales. Geophys. Res. Lett. 36, L22704.

Pretzsch, H., Biber, P., Schütze, G., Uhl, E., Rötzer, T., 2014. Forest stand growth dynamics in Central Europe accelerated since 1870. Nat. Commun. http://dx.doi.org/10.1038/ncomms5967.

Rasool, S.I., Schneider, S.H., 1971. Atmospheric carbon dioxide and aerosols: effects of large increases on global climate. Science 173, 138.

Ray, R.D., Douglas, B.C., 2011. Experiments in reconstructing twentieth-century sea-levels. Prog. Oceanogr. 91, 496.

Ring, M.J., Lindner, D., Cross, E.F., Schlesinger, M.E., 2012. Causes of the global warming observed since the 19th century. Atmos. Clim. Sci. 2, 401–415.

Rogelj, J., Meinshausen, M., Knutti, R., 2012. Global warming under old and new scenarios using IPCC climate sensitivity range estimates. Nat. Clim. Chang. 2, 248–253.

RSS, 2015. http://www.ssmi.com.

Salby, M.L., 2012. Physics of the Atmosphere and Climate. 2nd Edition. Cambridge University Press, Cambridge.

Scafetta, N., 2009. Empirical analysis of the solar contribution to global mean air surface temperature change. J. Atmos. Sol. Terr. Phys. 71, 1916.

Schlesinger, M.E., Ramankutty, N., 1994. An oscillation in the global climate system of period 65–70 years. Nature 367, 723.

Schwartz, S.E., 2012. Determination of earth's transient and equilibrium climate sensitivities from observations over the twentieth century: strong dependence on assumed forcing. Surv. Geophys. 33, 745–777.

SCRIPPS, 2014. http://scrippsco2.ucsd.edu/graphics_gallery/other_stations/global_stations_co2_concentration_trends.html.

Shaviv, N., 2015. How might climate be influenced by cosmic rays? Princeton Institute of Advance Studies Letter (Fall/Winter 2014–15)

Skeie, R.B., Berntsen, T., Aldrin, M., Holdren, M., Myhre, G., 2014. A lower and more constrained estimate of climate sensitivity using updated observations and detailed radiative forcing time series. Earth Syst. Dyn. 5, 139.

Sloan, T., Wolfendale, A.W., 2013. Cosmic rays, solar activity and the climate. Environ. Res. Lett. 8, 045022.

Spencer, R.W., Braswell, W.D., 2010. On the diagnosis of radiative feedback in the presence of unknown radiative forcing. J. Geophys. Res. 115, D16109.

Spencer, R.W., Christy, J.R., Braswell, W.D., 2015. www.drroyspencer.com/2015/04/version-6-0-of-the-uah-temperature-dataset-released-new-lt-trend-0-11-cdecade/.

Stevens, B., 2015. Rethinking the lower bound on aerosol radiative forcing. J. Clim. http://dx.doi.org/10.1175/JCLI-D-14-00656.1.

Stott, P.A., Forest, C.E., 2007. Ensemble climate predictions using climate models and observational constraints. Phil. Trans. R. Soc. A 365, 2029–2052.

Suess, H.E., 1980. The radiocarbon record in tree rings of the last 8000 years. Radiocarbon 22, 200–209.

Swanson, K.L., Tsonis, A.A., 2009. Has the climate recently shifted? Geophys. Res. Lett. 36, L06711.

Tomassini, L., Reichert, P., Knutti, R., Stocker, T.F., Borsuk, M.E., 2007. Robust Bayesian uncertainty analysis of climate system properties using Markov chain Monte Carlo methods. J. Clim. 20, 1239–1254.

UIUC, 2015. http://arctic.atmos.uiuc.edu/cryosphere/IMAGES/global.daily.ice.area.withtrend.jpg.

Volokin, D., ReLlez, L., 2015. Emergent model for predicting the average surface temperature of rocky planets with diverse atmospheres. Adv. Space Res. http://dx.doi.org/10.1016/j.asr.2015.08.006.

Vonder Harr, T.H., Bytheway, J.L., Forsythe, J.M., 2012. Weather and climate analyses using improved global water vapor observations. Geophys. Res. Lett. 39, L15802.

Wielicki, B.A., Wong, T., Allan, R.P., Slingo, A., Kiehl, J.T., Soden, B.J., Gordon, C.T., Miller, A.J., Yang, S.-K., Randall, D.A., Robertson, F., Susskind, J., Jacobowitz, H., 2002. Evidence for large decadal variability in the tropical mean radiative energy budget. Science 295, 841.

Wunsch, C., Heimbach, P., 2014. Bidecadal thermal changes in the abyssal ocean. J. Phys. Oceanogr. 44, 2013.

Zeng, N., Mariotti, A., Wetzel, P., 2005. Terrestrial mechanisms of interannual CO_2 variability. Glob. Biogeochem. Cycles 19, GB1016.

Zhen-Shan, L., Xian, S., 2007. Multi-scale analysis of global temperature changes and trend of a drop in temperature in the next 20 years. Meteorog. Atmos. Phys. 95, 115.